PROGRESS IN COLOR, COLORANTS AND COATINGS

available online @ www.pccc.icrc.ac.ir

Prog. Color Colorants Coat. 13 (2020), 177-185

Ministry of Science, Research and Technology
Institute for Color Science and Technology

Investigation of DSSCs Performance: The Effect of 1,8-naphthalimide Dyes and Na-doped TiO_2

M. Hosseinnezhad[1, 2*], M. Ghahari[3], H. Shaki[4], J. Movahedi[5]

[1.] Department of Organic Colorants, Institute for Color Science and Technology, P.O. Box: 16765-654, Tehran, Iran
[2.] Center of Excellence for Color Science and Technology, Institute for Color Science and Technology, P.O. Box 16765-654, Tehran, Iran
[3.] Department of Nanomaterials and Nanocoatings, Institute for Color Science and Technology, P.O. Box: 16765-654, Tehran, Iran
[4.] Department of Chemical Engineering, Faculty of Engineering, Golestan University, P.O. Box: 155, Aliabad Katoul, Iran.
[5.] Department of Physics, Shahrood University of Technology, P.O. Box: 36155-316, Shahrood, Iran

ARTICLE INFO

Article history:
Received: 16 Jul 2019
Final Revised: 22 Sep 2019
Accepted: 24 Sep 2019
Available online:23 Dec 2019

Keywords:
Dye-sensitized solar cells
Organic photosensitizer
Photovoltaic materials
Power conversion efficiencies
Na doped TiO_2.

ABSTRACT

In this paper, we selected three organic dyes based on 1,8-naphthalimide as photosensitizers for DSSCs preparation. The organic dyes were sensitized from acenaphthene as the starting material by standard reactions. Na-doped TiO_2 was prepared via one step hydrothermal method for preparation of dye-sensitized solar cells. Spectrophotometric measurements of the organic photosensitizers in DMF and on Na-doped TiO_2 substrate were carried out in order to study their maximum absorption wavelength. The maximum absorption wavelength for Dyes 1, 2 and 3 in DMF are 427, 434 and 435 nm and on TiO_2 films are 442, 446 and 446 nm, respectively. Finally, the proposed dyes were used as photosensitizer in a dye solar cell structure in the presence of Na-doped TiO_2 and their photovoltaic properties were investigated. The conversion efficiencies for the synthesized Dyes 1, 2 and 3 are 1.09%, 1.37% and 1.32%, respectively. Prog. Color Colorants Coat. 13 (2020), 177-185© Institute for Color Science and Technology.

1. Introduction

Dye-sensitized solar cells (DSSC) have attracted considerable attention due to their simple preparation procedure, architectural and environmental compatibility and good performance under diffuse light conditions [1-3]. The first fabricated DSSC was found to absorb visible light with wavelengths up to approximately 800 nm and the energy conversion efficiency of over 7%. In 2011, conversion efficiency of 11.4% was achieved by employing nanostructured semiconductor electrodes [4]. Recently, a conversion efficiency of 13% was reported by Mathew et al. [5] by using mesoporous semiconductor electrodes and porphyrin sensitizers. The basic components of DSSC include photo-anode, sensitizer, electrolyte, and counter electrode. Semiconductor nanostructures are employed to develop the photo-anode [6-9].

Akhtar and co-workers synthesized ZnO nanoparticles as photo-anode for DSSCs and achieved power conversion efficiency (PCE) of 4.1% [10]. They reasonably obtained good dye absorption of ~2.75 × 10^{-7} mol/cm^2 through the surface of ZnO Nanoparticle (NPs) thin film. Gholamrezaei et al. used sol–gel method to prepare $SrTiO_3$ nanostructures [11]. They investigated the effect of morphology and paste formation on cell efficiency. They obtained a PCE of 0.58% with fill factor (FF) of 59%. Das et al. used template method to fabricate TiO_2 photo-anode [12]. A

*Corresponding author: hosseinnezhad-mo@icrc.ac.ir

sol-gel method was employed to synthesize nano-porous TiO_2. In this method, dextran (TNPO-D) and glucose (TNPO-G) were used as templates. Calcination process caused the decomposition of templating agents and formation of 10 nm nano-pores in TiO_2 which was then employed in DSSCs. They obtained PCE of 4.1% and 3.7% for TNPO-D and TNPO-G, respectively.

Zhu et al. reported two new sensitizers based on triphenylamine-dicyanovinylene and used for p-type dye-sensitized solar cells [13]. This study suggested that amendment of the bridging moiety among triphenyl amine and the carboxylic group by cumulative thiophene units is a promising way for averting charge recombination and hence power conversion efficiency can be boosted. Four new organic dyes were synthesized by Reddy et al. [14]. The dyes had electron rich thiophene spin-offs as antennas and cyanoacrylic acid as acceptor, bridged by phenothiazine or phenoxazine. The light harvesting ability of the dyes could be improved by the alkyl substituted thiophene units. Movahedi et al. designed and synthesized free-metal dyes based on indoline [15]. The proposed dyes were synthesized from phenothiazine as the starting material by standard reactions. The conversion efficiency for the synthesized dye was 0.92%.

In this paper, an attempt has been made to prepare DSSC using Na-doped TiO_2 as photo-anode and indoline-based organic dyes as sensitizer. The fabricated DSSC was studied for its structure and efficiency using platinum as the catalyst for counter electrode and iodide-triiodide as electrolyte. The spectrophotometric properties of the organic dyes in solution and on a nanoanatase TiO_2 substrate and electrochemical measurements were examined. The cyclic voltammetry (CV) data were used to determine the highest occupied molecular orbital, lowest unoccupied molecular orbital levels and band gap of the organic dyes. The structure of the dye molecules are shown in Figure 1.

2. Experimental

2.1. Materials and instrumentation

All compounds used in this study were of analytical grade unless otherwise stated. The synthesis route and full characterization of the intermediates, organic dyes and nano-particles are described elsewhere [16, 17]. UV-visible spectrophotometry was carried out on a Cecil 9200 double beam transmission spectrophotometer to obtain molar extinction coefficients and absorption maxima.

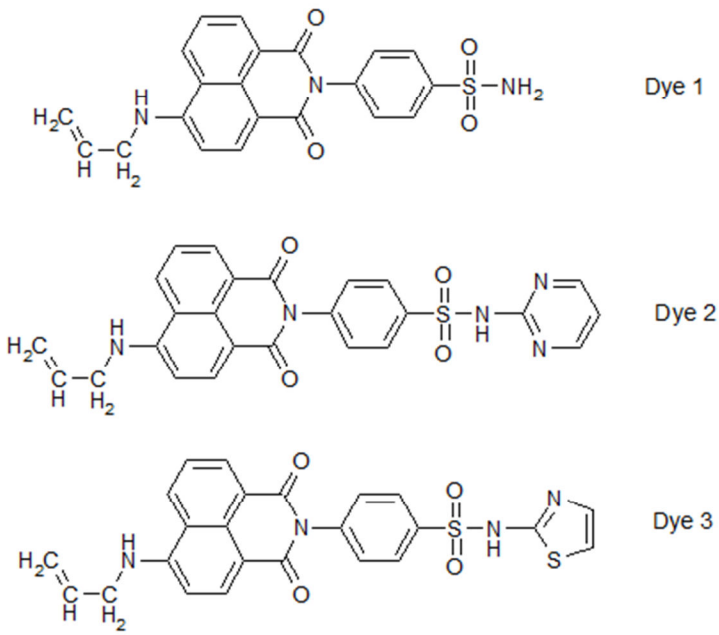

Figure 1: Chemical structure of the organic dyes.

2.2. General procedure for fluorescent dyes preparation

The solution of 4-nitro-N-aminobenzensulfonamode-1,8-naphthalimide, 4-nitro-N-4-amino-N-2-thiazoyl-benzenesulfonamide-1,8-naphthalimide and 4-nitro-N-4-amino-N-(2-pyrimidinyl) benzenesulfonamide-1,8-naphthalimide as intermediates (5 mmol) was prepared in 30 mL DMF. Then allylamine (5 mmol) was added to the solution at room temperature separately. After 24 h, the final stage of reaction was controlled by TLC in a solvent system n-hexane/acetone (1:1). The resulting solutions were poured into 300 mL water. The precipitations were filtered off, washed with water and dried. Recrystallization from ethanol offered the dyes 1-3 as orange crystals.

2.3. Electrochemical measurements

Electrochemical measurements of the synthesized dyes were carried out in solution in acetonitrile. The oxidation potential (E_{ox}) was measured using three small-sized electrodes. Ag quasi reference electrode (QRE) was used as the reference. Platinum wires were used as the photo-anode and counter electrode. All electrode potentials were calibrated with respect to ferrocene (Fc)/ferrocenium (Fc^+) redox couplet. An acetonitrile solution of each dye containing tetrabutylammonium perchlorate (0.1 mol dm^{-3}) and ferrocene (ca. 1 mmol dm^{-3}) was prepared. The electrochemical measurements were performed at a scan rate of 100 mV s^{-1} [18, 19].

2.4. Assembly of dye-sensitized solar cells (DSSCs) and photovoltaic characterization

A nanocrystalline film was coated on a transparent FTO/glass substrate. The dye was adsorbed by dipping the coated FTO/glass in a 5×10^{-5} M ethanolic solution of the dye containing 7% 4-tert-butylpyridine and 50 mM 3α,7α-dihydroxy-5β-cholic acid (cheno) for 12 h. The visible bands in the absorption spectrum of the dyes after adsorption on the nanocrystalline film only appeared after the work electrodes were dipped in the dye solution for at least 12 h. The presence of 4-tert-butylpyridine and cheno is necessary to avoid surface aggregation of the sensitizer. Finally, the film was washed with acetonitrile-ethanol 1:1 mixed solution. Acenonitrile-ethylene carbonate (v/v=1:4) containing tetrabutyl ammonium iodide (0.5 mol dm^{-3}) was used as the electrolyte. The dye-adsorbed nanocrystalline electrode, the Pt counter electrode and the electrolyte solution were assembled into a sealed sandwich type solar cell [20-23].

Photovoltaic properties were measured under monochromatic light with a constant photon number (5×10^{15} photon cm^{-2} s^{-1}). J-V characteristics were measured under illumination with AM 1.5 simulated sun light (100 mW cm^{-2}) through a shading mast (5.0 mm×4 mm) by using a Bunko-Keiki CEP-2000 system.

3. Results and Discussion

The starting material for the preparation of naphthalimide derivatives was 4-nitro-1,8-naphthalic anhydride. The synthesized dyes were prepared by imidation, reduction and allylation reactions from 4-nitro-1,8-naphthalic anhydride. The imidation of aromatic cyclic anhydrides occurs through nucleophilic substitution mechanism, in which the reaction of the attacking amine is carried out in an acetic acid under a reflux condition. For preparing 4-nitro-N-substituted-1,8-naphthalimide, 4-nitro-1,8-naphthalic anhydride was reacted with the corresponding amine and the completion of the reaction was controlled by TLC. Preparation of 4-amino(allylamino)-N-substituted-1,8-naphthalimide as an intermediate plays significant role in the naphthalimide dyes and colored polymer series. Reduction of 4-nitro-N-substituted-1,8-naphthalimides with tin(II) chloride and hydrochloric acid in ethanol as the solvent gave 4-amino-N-substituted-1,8-naphthalimides. 4-Allylamino-N-substituted-1,8-naphthalimides were synthesized by the reaction of 4-nitro-N-substituted-1,8-naphthalimides with allylamine in DMF as the solvent. The yields of 4-amino(allylamino)-N-substituted-1,8-naphthalimides [16, 24, 25].

The maximum absorption wavelength (λ_{max}) and the molar extinction coefficients (ε_{max}) for the synthesized dye in DMF are shown in Table 1 and Figure 2, together with the λ_{max} of the corresponding dyes adsorbed on the Na/TiO_2 film. The absorption peaks at organic can be assigned to an intra-molecular charge transfer between the donor and acceptor groups [26], providing an efficient charge-separation for the excited state. For the organic dyes, when an extra electron acceptor was linked to the vinyl bridge, the λ_{max} had a bathochromic shift [27, 28]. This shift in the maximum absorption peak arises from the fact that more stronger electron acceptor of two aromatic rings the overall electron withdrawing ability of the system and hence lowering the level of the lower unoccupied molecular orbital (LUMO), thus reducing the

gap between the higher unoccupied molecular orbital (HOMO) and the LUMO states [18, 29]. Upon dye adsorption onto the photo-anode surface, the maximum absorption wavelength is bathochromically shifted as compared to the corresponding spectra in solution, implying that dyes adsorbed onto the photo-anode surface contain partial J-type aggregates [24, 27]. The molar extinction coefficients of Dyes 1, 2 and 3 in DMF at their respective λ_{max} are also shown in Table 1, indicating that these novel dyes have good light harvesting abilities.

The fluorescent characteristics of the dyes measured in DMF are represented in Table 1. In DMF solution, dyes show fluorescence due to the charge transfer from the electron-donating group to the acceptor group. The maximum fluorescence emission of the dye in DMF is 527.5 nm. The absorption maxima (λ_{max}) of the fluorescent dyes were in the visible region (427–435 nm), while the fluorescence emission (λ_F) was observed in the region of 526–527.5 nm. Data presented in Table 1 showed that different substituents at the N-imide and C-4 positions have a small effect on the fluorescence maxima (λ_F).

The oxidation potential (E_{ox}) of organic dye was measured in solution by cyclic voltammetry [18, 19]. There are two distinct redox waves observed in the voltammogram. The first oxidative wave (I) was due to the oxidation of the internal standard of ferrocene, whereas the second wave (II) near was due to the electrochemical oxidation of dyes [22, 32]. Although the standard E_{ox} value is usually not easily obtained experimentally, it can be approximately estimated from the cyclic voltammetric peak potential method.

The standard and estimated E_{ox} values will be equal if the electrochemical oxidation is a reversible step [33-36]. The electrochemical properties are listed in Table 2. The CV curves of organic dyes are presented in Figure 3.

Table 1: Absorption properties of the organic dyes.

Dye	λ_{max} (nm)[a]	ε ($M^{-1}cm^{-1}$)	λ_{max} (nm)[b]	λ_F (nm)[a]
1	427	12362	442	527.5
2	434	13289	446	526
3	435	13019	446	527

a) in DMF solution, b) on photo-anode substrate

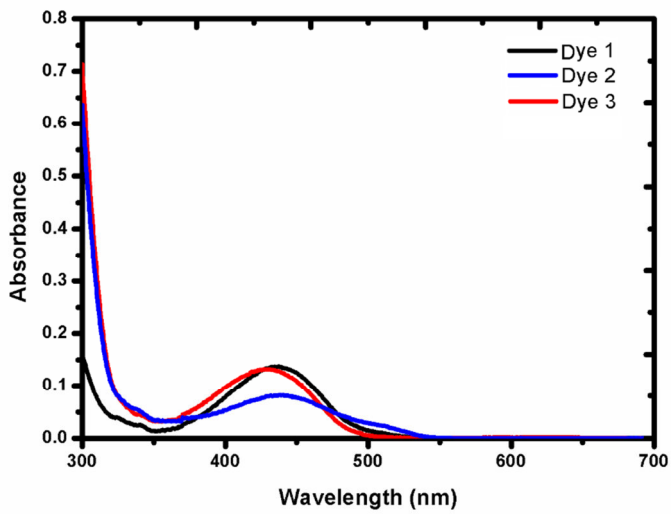

Figure 2: UV-Vis spectra of organic dyes.

Table 2: Electrochemical properties of the organic dyes.

Dye	E_{pa} (V)	$E_{0\text{-}0}$ (V)	E_{LUMO} (V)
1	0.84	2.09	-1.25
2	0.90	2.22	-1.32
3	0.91	2.21	-1.30

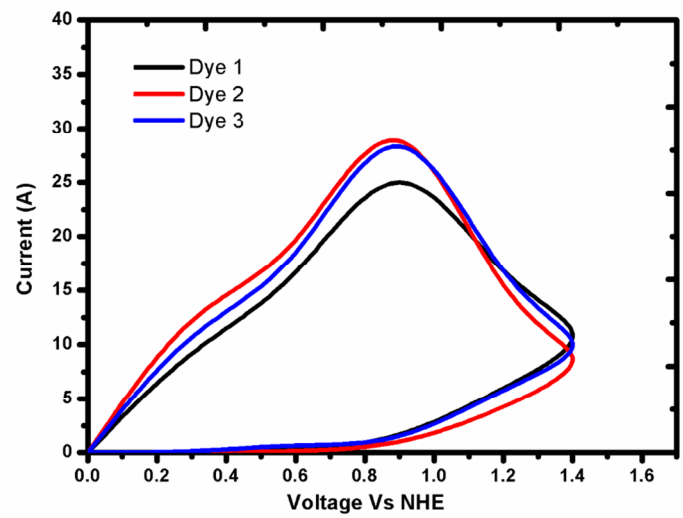

Figure 3: CV curves of the organic dyes.

X-ray diffraction pattern of Na-doped TiO_2 film is shown in Figure 4. It can be seen that all the peaks at 27.39°, 36.08°, 39.10°, 41.3°, 43.97°, 54.36°, and 56.68° correspond to rutile TiO_2 phase according to JCPDS 01-088-1173. Remarkable amount of NaCl phase is also observed beside the rutile phase which may be due to insufficient washing process. A low amount of Na ions doped in the titan phase and residue has remained as NaCl phase. In addition, the sample contains a low amount of anatase TiO_2 phase.

The morphological features of undoped and Na-doped TiO_2 samples were examined using FESEM (Figure 5). Figure 5 shows the formation of TiO_2 nanoparticles and NaCl particles synthesized via hydrothermal method. It can be seen that most of the nanoparticles are cubic, however, there are some irregular TiO_2 and rod shape NaCl particles. As can be seen in Figure 5, doping of TiO_2 by sodium has no remarkable effect on the morphology of TiO_2 particles. However, it seems that the average size of TiO_2 particles has reduced after doping. The average particle size of TiO_2 is less than 200 nm. The EDX analysis of two different morphologies reveals that the rod shape particles are NaCl and the others are TiO_2 [17, 36].

Dye-sensitized solar cells (DSSCs) were constructed and compared in order to clarify the relationships between the sensitizing behavior of organic dye molecules and Na-doped TiO_2 thin films. This dye was used in DSSCs as sensitizer for nanocrystalline anatase TiO_2 and Na-doped TiO_2. A typical photocurrent–photovoltage (J–V) curve for a cell based on organic dye is depicted in Figure 6. The detailed photovoltaic parameters are also summarized in Table 3. The solar energy to electricity conversion efficiency (η) of the DSSCs is calculated from short circuit current (J_{sc}), open-circuit photovoltage (V_{oc}), fill factor (FF), and the intensity of the incident light (P_{in}) [37].

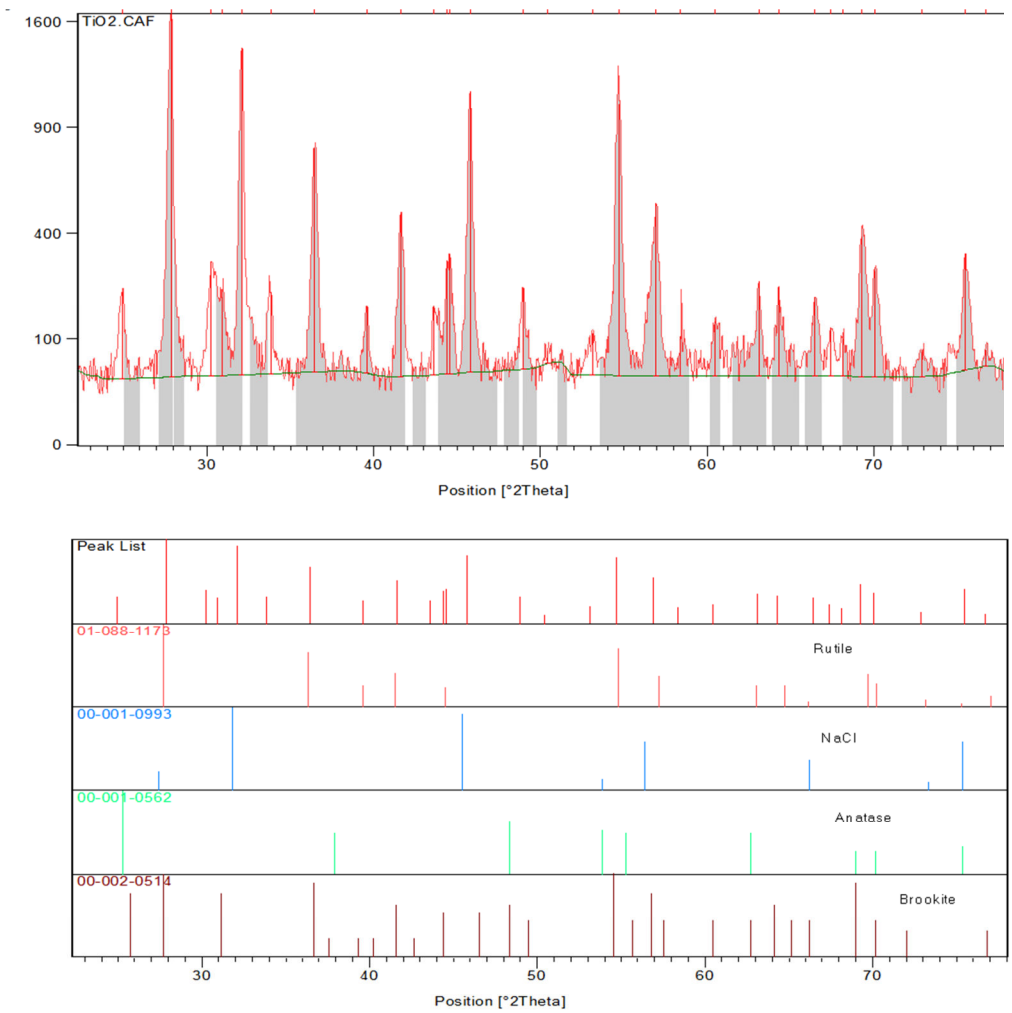

Figure 4: X-ray diffraction pattern of undoped and Na-doped TiO_2 films.

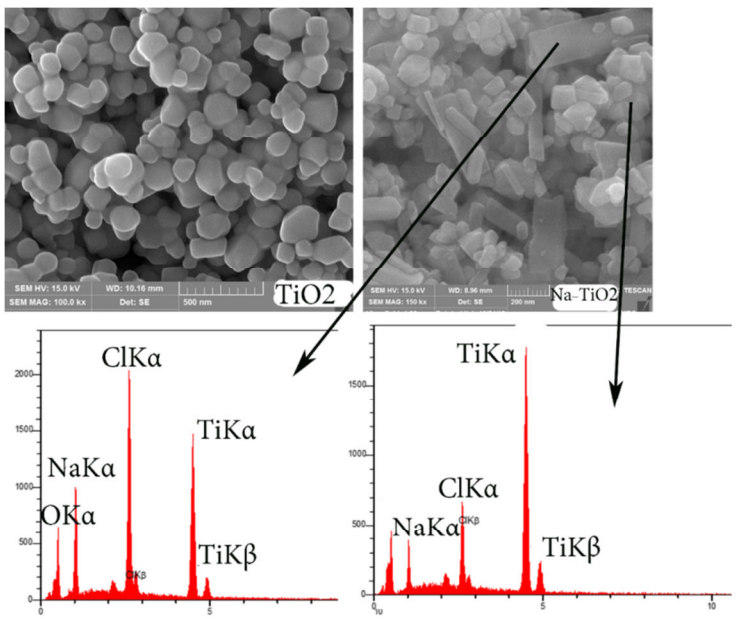

Figure 5: FESEM images of Na-doped TiO_2 nanostructures.

Table 3: Photovoltaic performance of DSSCs based on organic dyes.

DSSCs based on TiO_2				
Dye	V_{OC} (V)	J_{SC} (mA.cm^{-2})	FF	η (%)
1	0.58	3.59	0.57	1.19
2	0.57	4.19	0.57	1.34
3	0.56	4.01	0.57	1.28
DSSCs based on Na doped TiO_2				
Dye	V_{OC} (V)	J_{SC} (mA.cm^{-2})	FF	η (%)
1	0.52	3.69	0.57	1.09
2	0.55	4.38	0.57	1.37
3	0.54	4.31	0.57	1.32

According to the results shown in Table 3, under the standard global AM 1.5 solar conditions, the conversion efficiencies of solar cells containing organic dye (Dyes 1, 2 and 3) based on TiO_2 are 1.19%, 1.34% and 1.28%, respectively. The efficiencies of solar cells containing organic dye (Dye 1-3) based on Na-doped TiO_2 are 1.09%, 1.37% and 1.32%, respectively. The conversion efficiency of the device is probably due to the stronger electron withdrawing ability of the combined cyanine acceptor groups [38]. The efficiency of converting solar energy to electricity by the present organic dyes could be improved by extending the conjugated length of the organic dyes or by incorporation of a thiophene π-bridge [37, 38].

It can be seen from the photovoltaic results that the overall conversion efficiency of DSSCs sensitized by Dyes 2 and 3 in the presence of Na-doped TiO_2 is higher than DSSCs based on undoped TiO_2 nano-particles. The improved performance of Na-doped TiO_2 based DSSC could be attributed to the enhancement in optical properties of the sample by decreasing the intrinsic defects. Introduction of dopant (Na^+) to TiO_2 lattice will lead to a downward shift in flat band voltage. This in turn enhances the electron injection rate from LUMO of dye to the conduction band of TiO_2 which improves the overall DSSC efficiency [17, 36].

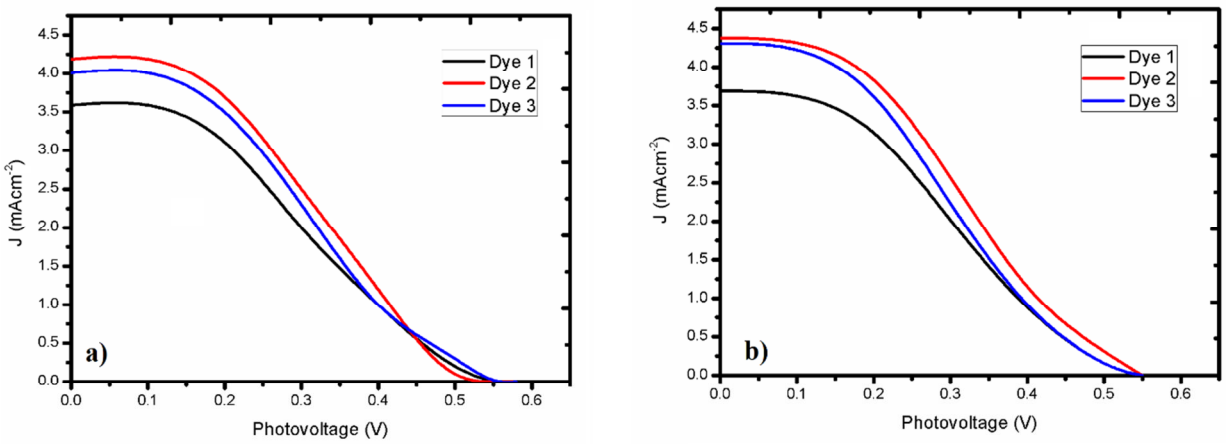

Figure 6: Current density-voltage characteristics for a) TiO_2 and b) Na-doped TiO_2.

4. Conclusions

Three metal-free organic dyes with D-π-A structure were utilized as photosensitizer in dye-sensitized solar cells devices. Na-doped TiO_2 was synthesized via one-step hydrothermal method successfully for preparation of dye-sensitized solar cells. The spectrophotometric properties of the organic dyes in solvent and on Na-doped TiO_2 films were examined. The absorption maxima of synthesized dyes applied on the surface of Na-doped TiO_2 film gave a bathochromic effect compared to the corresponding dye spectra in solution. Finally, the organic dyes were utilized in DSSCs and their photovoltaic behaviors were assessed. Solar energy to electricity conversion efficiencies of 1.19%, 1.34% and 1.28% were achieved for synthesized dyes 1, 2 and 3 in DSSCs based on TiO_2, respectively. Solar energy to electricity conversion efficiencies of 1.09%, 1.37% and 1.32% were achieved for synthesized dyes 1, 2 and 3 in DSSCs based on Na-doped TiO_2, respectively. The results showed that the overall conversion efficiencies of DSSCs sensitized by Dyes 2 and 3 in the presence of Na-doped TiO_2 is higher than DSSCs based on undoped TiO_2 nano-particles due to the enhancement in optical properties of the sample by decreasing the intrinsic defects.

Acknowledgement

The authors sincerely thank the Center of Excellence for Color Science and Technology for making this investigation possible.

5. References

1. S. Shalini, R. Balasundaraprabhu, S. Prasanna, T. K. Mallick, S. Senthilarasu, Review on natural dye sensitized solar cells: Operation, materials and methods, *Renew. Sustain. Energy Rev.*, 51(2015), 1306-1325.
2. M. Hosseinnezhad, H. Shaki, Investigation of Photovoltaic Properties of 1,8-Naphthalimide Dyes in Dye-sensitized Solar Cells, *Prog. Color Colorants Coat.*, 11(2018), 253-258.
3. M. Ataeefard, S.M. Sadati Tilebon, M.R. Saeb, Intelligent modelling and optimization of emulsion aggregation method for producing green printing ink, *Green Process. Synth.*, 8(2019), 703-718.
4. S. Suhaimi, M.M. Shahimin, Z.A. Alahmed, J. Chysky, A.H. Reshak, Materials for enhanced dye-sensitized solar cell performance: electrochemical application, *Int. J. Electrochem. Sci.*, 10 (2015), 2859–2871.
5. S. Mathew, A. Yella, P. Gao, R. Humphry-Baker, F. Basile, E. Curchod, N. A. Stani, Dye-sensitized solar cells with 13% efficiency achieved through the molecular engineering of porphyrin sensitizers, *Nat. Chem.*, 6(2014), 242–247.
6. V. Sugathan, E. John, K. Sudhakar, Recent improvements in dye sensitized solar cells: A review, *Renew. Sustain. Energy Rev.*, 52(2015), 54-64.
7. M.S. Akhtar, A facile synthesis of ZnO nanoparticles and its application as photoanode for dye sensitized solar cells, *Sci. Adv. Mater.*, 7(2015), 1137 – 1142.
8. S. Gholamrezaei, M. Salavati Niasari, M. Dadkhah, B. Sarkhosh, New modified sol – gel method for preparation $SrTiO_3$ nanostructures and their application in dyesensitized solar cells, *J. Mater. Sci.: Mater. Electron.,* 27(2016), 118 – 125.
9. M. Hosseinnezhad, H. Shaki, Investigation of photovoltaic properties of dye-sensitized solar cells based on azo dyes contain various anchoring groups, *Pigm. Resin Technol.*, 48(2019), 481-486.
10. T.K. Das, P. Ilaiyaraja, C. Sudakar, Template assisted nanoporous TiO_2 nanoparticles: the effect of oxygen vacancy defects on photovoltaic performance of DSSC and QDSSC, *Sol. Energy*, 159(2018), 920 – 929.
11. L. Zhu, H. Bin Yang, C. Zhong, C. Ming Li, Rational design of triphenylamine dyes for highly efficient p-type dye sensitized solar cells, *Dye Pigm.*, 105(2014), 97-104.
12. M.A. Reddy, B. Vinayak, T. Suresh, S. Niveditha, K. Bhanuprakash, S.P. Singh, A. Islam, L. Han, M. Chandrasekharam, Highly conjugated electron rich thiophene antennas on phenothiazine and phenoxazine-based sensitizers for dye sensitized solar cells, *Synth. Met.*, 195(2014), 208-216.
13. J. Movahedi, M. Hosseinnezhad, H. Haratizadeh, N. Falah, Synthesis and investigation of photovoltaic properties of new organic dye in solar cells device, *Prog. Color Colorants Coat.*, 12(2019), 33-38.
14. H. Shaki, A. Khosravi, K. Gharanjig, A. Mahboubi, Investigation of synthesis, characterization, photophysical and biological properties of novel antimicrobial fluorescent naphthalimide derivatives, *Mater. Technol.: Adv. Performance Mater.*, 31(2016), 322-331.
15. S. Shalini, R. Balasundaraprabhu, T. Satish Kumar, K. Sivakumaran, M.D. Kannan, Synergistic effect of sodium and yeast in improving the efficiency of DSSC sensitized with extract from petals of Kigelia Africana, *Optical Mater.*, 79(2018), 210-219.
16. M. Hosseinnezhad, S. Moradian, K. Gharanjig, S. Rouhani, M. Ataeefard, Investigating the Effect of Substrate Photo-Electrode Based on Screen Method

on Performance of Dye-Sensitized Solar Cells, *Prog. Color. Colorants Coat.*, 11(2018), 47-54.
17. M. Hosseinnezhad, S. Rouhani, K. Gharanjig, Extraction and application of natural pigments for fabrication of green dye-sensitized solar, *Opto-Electron. Rev.*, 26(2018), 165-171.
18. X. Liu, C. Li, X. Peng, Y. Zhou, Z. Zeng, Y. Li, T. Zhang, B. Zhang, Y. Dong, D. Sun, P. Cheng, Y. Feng, Performance of four artificial chlorin-type sensitizers with different stereostructures in dye-sensitized solar cells, *Dye Pigm.*, 98(2013), 181-189.
19. M. Hosseinnezhad, S. Rouhani, Characteristics of nanostructure dye-sensitized solar cells using food dyes, *Opto-Electron. Rev.*, 24(2016), 34-39.
20. M. Hosseinnezhad, S. Moradian, K. Gharanjig, Novel organic dyes based on thioindigo for dye-sensitized solar cells, *Dye Pigm.*, 123(2015), 147-153.
21. M. Hosseinnezhad, A. Khosravi, K. Gharanjig, S. Moradian, The comparison of spectra and dyeing properties of new azonaphthalimide with analogues azobenzene dyes on natural and synthetic polymers, *Arabian J. Chem.*, 10(2017), s3284-s3291.
22. I. Ajaj, F. H. Assaleh, J. Markovski, M. Rancic, D. Brkovic, M. Milcic, A. D. Marinkovic, Solvatochromism and azo–hydrazo tautomerism of novel arylazo pyridone dyes: Experimental and quantum chemical study, *Arabian J. Chem.*, (2015), doi.org/10.1016/j.arabjc.2015.08.029.
23. M. Hosseinnezhad, Enhanced performance of dye-sensitized solar cells using perovskite DSSCs tandem design, *J. Electron. Mater.*, 48(2019), 5403-5408.
24. S. Shalini, R. Balasundaraprabhu, S. Prasanna, T.K. Mallick, S. Senthilarasu, Review on natural dye sensitized solar cells: Operation, materials and methods, *Renew. Sustain. Energy Rev.*, 51(2015), 1306-1325.
25. Y.J. Kim, S. Mathew, M. Gratzel, T. Torres, M.K. Nazeeruddin, Molecular Engineering of Phthalocyanine Sensitizers for Dye-Sensitized Solar Cells, *J. Phys. Chem. C*, 118(2018), 17166-17170.
26. M. Hosseinnezhad, K. Gharanjig, S. Moradian, M. R. Saeb, In quest of power conversion efficiency in nature-inspired dye-sensitized solar cells: Individual, co-sensitized or tandem configuration?, *Energy*, 134(2017), 864-870.
27. C. Chen, M. Cheng, X. Ding, H. Li, F. Qiao, L. Xu, H. Li, H. Li, Molecular engineering of triphenylamine functionalized phenoxazine sensitizers for highly efficient solid-state dye sensitized solar cells, *Dye Pigm.*, 162(2019), 606-610.
28. M. Hosseinnezhad, K. Gharanjig, Investigation of photovoltaic properties of nanostructure indoline dye-sensitised solar cells using changes in assembling materials, *Pigment Resin Technol.*, 46(2017), 393-398.
29. M. Hosseinnezhad, S. Rouhani, Synthesis and application of new fluorescent dyes in dye-sensitized solar cells, *Appl. Phys. A*, 123(2017), 694-703.
30. M. Matsui, T. Fujita, Y. Kubota, K. Funabiki, J. Jin, T. Yoshida, H. Miura, Substituent effects in a double rhodanine indoline dye on performance of zinc oxide dye-sensitized solar cell, *Dyes Pigm.*, 86(2010), 143-8.
31. K. Hara, T. Sato, R. Katoh, A. Furube, Y. Ohga, A. Shinpo, Molecular Design of Coumarin Dyes for Efficient Dye-Sensitized Solar Cells, *J. Phys. Chem. B*, 107(2003), 597-606.
32. C. Shen, Y. Wu, W. Zhang, H. Jiang, H. Zhang, E. Li, B. Chen, X. Duan, W. Zhu, Incorporating quinoxaline unit as additional acceptor for constructing efficienct donor-free solar cells sensitizers, *Dyes Pigm.*, 149(2018), 65-72.
33. S. Shalinia, N. Prabavathy, R. Balasundaraprabhu, T. Satish Kumarc, D. Velauthapillai, P. Balraju, S. Prasanna, Studies on DSSC encompassing flower shaped assembly of Na-doped TiO_2 nanorods sensitized with extract from petals of Kigelia Africana, *Optik*, 155(2018), 334-343.
34. H. Cheng, Y. Wu, J. Su, Z. Wang, R.P. Ghimire, M. Liang, Z. Sun, S. Xue, Organic dyes containing indolodothienpyrrole unit for dye-sensitized solar cells, *Dyes Pigm.*, 149(2018), 16-24.
35. I. Duerto, E. Colom, J.M. Andres Castan, S. Franco, J. Garin, J. Orduna, B. Villacamparr, M.J. Blesa, DSSCs based on aniline derivatives functionalized with a tert-butyldimethylsilyl group and the effect of the π-spacer, *Dyes Pigm.*, 148(2018), 61-71.
36. H. Wei, J. Shen, Y. Liu, T. Huang, Q. Zhang, J. Zhao, X. Zhao, Synthesis and properties of organic sensitizers bearing asymmetric double donor π-acceptor chains for dye-sensitized solar cells, *Dye Pigm.*, 149(2018), 789-795.
37. L. Michelão Martins, S. de Faria Vieira, G.B. Baldacim, Bruna, A. Bregadiolli, J. Cláudio Caraschi, A. Batagin-Neto, L. Carlos da Silva-Filho, Improved synthesis of tetraaryl-1,4-dihydropyrrolo[3,2-b]pyrroles a promising dye for organic electronic devices: An experimental and theoretical approach, *Dye Pigm.*, 148(2018), 81-90.
38. M. Wendel, A. Kumorkiewicz, S. Wybraniec, M. Ziółek, G. Burdziński, Impact of S1→S0 internal conversion in betalain-based dye sensitized solar cells, *Dyes Pigm.*, 141(2017), 306-315.

How to cite this article:
M. Hosseinnezhad, M. Ghahari, H. Shaki, J. Movahedi, Investigation of DSSCs Performance: The Effect of 1,8-naphthalimide Dyes and Na-doped TiO_2. Prog. Color Colorants Coat., 13 (2020), 177-185.